POLITECNICO DI TORINO
Repository ISTITUZIONALE

ADVANCED TAILORED KINEMATIC MODELS FOR MULTI-FIELD ANALYSIS OF LAMINATED STRUCTURES

Original
ADVANCED TAILORED KINEMATIC MODELS FOR MULTI-FIELD ANALYSIS OF LAMINATED STRUCTURES / Zappino, E., Carrera, E., Scano, D.. - ELETTRONICO. - (2025), pp. 42-52. (11th ECCOMAS Thematic Conference on Smart Structures and Materials Linz (Austria) 1-3 Luglio 2025) [10.7712/150125.13614.100005].

Availability:
This version is available at: 11583/3014696 since: 2026-08-20T15:59:01Z

Publisher:
ECCOMAS Proceedia

Published
DOI:10.7712/150125.13614.100005

Terms of use:

This article is made available under terms and conditions as specified in the corresponding bibliographic description in the repository

Publisher copyright

(Article begins on next page)

23 September 2026

Available online at www.eccomasproceedia.org
Eccomas Proceedia SMART (2025) 42-52

ECCOMAS
Proceedia

XI ECCOMAS Thematic Conference on Smart Structures and Materials - SMART 2025
M. Krommer, M. Nader and M. Schagerl (Eds)

Received: 19 April 2025 / Revised: 29 August 2025 / Accepted: 7 October 2025
© The Author(s) 2025

Advanced Tailored Kinematic Models for Multi-Field Analysis of Laminated Structures

Enrico Zappino, Erasmo Carrera, Daniele Scano

Abstract. This paper presents a novel methodology for constructing beam theories with fully customizable kinematic fields specifically designed for multi-layered composite piezoelectric structures. This work extends the most recent Carrera Unified Formulation implementations for multi-field analyses of piezoelectric structures, optimizing computational resources while maintaining accuracy. The proposed method applies Layer-Wise expansions where necessary, such as for the electric field, while employing Equivalent Single Layer formulations for fields that do not require piece-wise accuracy, like in-plane displacements. This tailored kinematic approach balances computational cost and accuracy, ensuring a more efficient yet precise structural analysis. This strategy is particularly effective for complex laminated structures, where different physical fields require varying levels of detail. Numerical analyses confirm the effectiveness of the approach, demonstrating its ability to provide accurate and efficient multi-field simulations. By selecting appropriate kinematic formulations for each field, the proposed method achieves high-fidelity modeling while significantly reducing computational costs.

Key words: Finite element method, higher-order theories, kinematic models, Unified Formulation, multifield analysis

1 INTRODUCTION

Piezoelectric materials exhibit a unique two-way energy conversion capability between mechanical and electrical domains. Certain crystals generate electrical charges when mechanically deformed - a linear relationship now known as the direct piezoelectric effect. The reciprocal phenomenon, termed the converse piezoelectric effect, describes mechanical deformation induced by applied electric fields. In smart structure applications, piezoelectric actuators exploit the converse effect to generate controlled strains. As demonstrated in seminal works by Crawley and Luis [1], Bailey and Hubbard [2], and Robbins and Reddy [3], these induced strains contribute additively to the total strain field of host structures. Notably, Crawley and Luis [1] developed a comprehensive analytical framework capable of modeling both surface-bonded and

Enrico Zappino & Erasmo Carrera & Daniele Scano
MUL2 Lab, Department of Mechanical and Aerospace Engineering, Politecnico di Torino, 10129 Turin, Italy
e-mail: enrico.zappino@polito.it, erasmo.carrera@poltio.it, daniele.scano@polito.it

ISSN:3078-543X. Published by Eccomas Proceedia.
Peer-review under responsibility of the organizing committee of SMART 2025.
doi: 10.7712/10.7712/150125.13614.100005

embedded piezoelectric actuators in beam structures.
The work of Sarvanos and Heyliger [4] provides a comprehensive review and systematic classification of piezoelectric theories based on their underlying kinematic assumptions. To address the inherent limitations of analytical approaches, researchers have increasingly adopted finite element (FE) formulations for modeling piezoelectric composite structures. The active vibration control of smart structures has been investigated through both three-dimensional and reduced-order modeling approaches. While Dong *et al.* [5] employed 3D solid elements for plate analyses, numerous studies (e.g., Umesh and Ganguli [6]) have utilized classical Kirchhoff-Love theory, which neglects transverse shear deformation effects. To address this limitation, first-order shear deformation theory (FSDT) implementations (Kumar and Narayanan [7]; Vasques and Rodrigues [8]) have incorporated transverse shear effects. Moita *et al.* [9] developed an advanced triangular plate/shell element featuring 24 degrees of freedom and additional electrical potential degrees of freedom per piezoelectric layer. A third-order shear deformation theory is adopted. Beheshti-Aval *et al.* [10] introduced a three-node piezoelectric beam element based on a refined sinusoidal model that inherently accounts for transverse shear deformation without requiring shear correction factors. Finally, the Carrera Unified Formulation (CUF) has been introduced [11, 12]. This framework permits to generate beam and plate theories with the freedom to use the desired structural models.
The majority of existing studies adopt the Equivalent Single Layer (ESL) approach for modeling composite structures, where field variables are expressed independently of the laminate's layer count. For higher-fidelity analyses requiring through-thickness resolution, the Layer-Wise (LW) approach becomes necessary, assigning independent variables to each material layer. However, this enhanced accuracy comes at a substantially increased computational expense, prompting ongoing research to develop balanced efficiency-accuracy formulations. A notable contribution by Ballhause *et al.* [13] presents a unified electro-mechanical formulation for smart multilayered plates that encompasses both ESL and LW modeling paradigms and utilizes variable kinematic expansions up to fourth-order.
Recent research demonstrates the ability to create precise, customized models for predicting complex structural behaviour. However, traditional approaches require recalculating governing equations for each new theory. To address this, unified frameworks like Generalized Beam Theory [14] and the CUF have been developed, allowing flexible selection of multiple model types within a single framework. While existing methods show promise, they fail to evaluate the individual contributions of each term in the expansion. This study proposes a consistent formulation that enables users to choose theories with tailored precision. Given the importance of computational efficiency in structural analysis, the research seeks to balance accuracy and cost-effectiveness. Specifically, it investigates the combined use of ESL and LW approaches within unified structural models. This work extends the methodology proposed by Carrera and collaborators [15, 16, 17] for the pure mechanical cases.
This paper is organized as follows: (a) Section 2 presents the theoretical foundations of the Unified Formulation for beam structures and the approximations for the generalized displacements. (b) Section 3 derives the governing equations for piezoelectric materials within this

framework. (c) Section 4 demonstrates the methodology through a detailed stiffness matrix assembly procedure. (d) Section 5 presents numerical results validating the accurate prediction of both displacements and stress fields. (e) Section 6 summarizes key findings and discusses promising directions for future research.

2 CARRERA UNIFIED FORMULATION

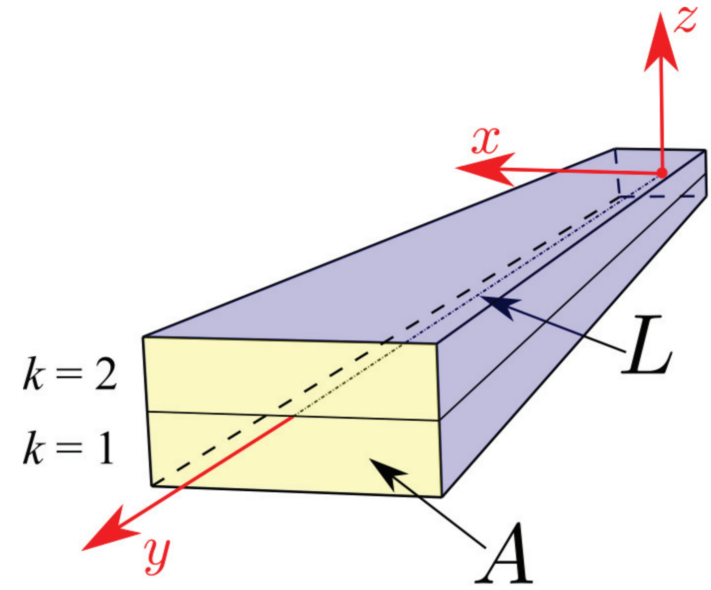

Figure 1: Reference systems for beam structures.

Figure 1 illustrate generic beam and the reference system. The upperscript k indicates the layer. The generalized electromechanical displacement vector field (with u_ϕ as the electric potential) may be expressed as follows:

$$\mathbf{u}^k(x,y,z) = \left\{ \; u_x^k(x,y,z), \quad u_y^k(x,y,z), \quad u_z^k(x,y,z), \quad u_\phi^k(x,y,z) \; \right\}^T \tag{1}$$

In the 1D beam formulation, the basis functions, $F_\tau(x,z)$, are defined over the $x-z$ plane. The following expressions can be utilized for each component:

$$f^k(x,y,z) = F_\tau^k(x,z) f_\tau^k(y), \qquad \tau = 1,2,...,M \tag{2}$$

The formulation employs Einstein's summation convention. This framework enables the displacement field to be expressed using general basis functions. To handle geometrically complex structures and diverse boundary conditions, the FEM is implemented.

$$
\begin{aligned}
u_x^k(x,y,z) &= N_i(y)F^k_{u_x\tau}(x,z)q^k_{x_{\tau i}} \quad \text{with} \;\; \tau = 1,\dots,M_{u_x} \quad i = 1,\dots,N_n \\
u_y^k(x,y,z) &= N_i(y)F^k_{u_y\tau}(x,z)q^k_{y_{\tau i}} \quad \text{with} \;\; \tau = 1,\dots,M_{u_y} \quad i = 1,\dots,N_n \\
u_z^k(x,y,z) &= N_i(y)F^k_{u_z\tau}(x,z)q^k_{z_{\tau i}} \quad \text{with} \;\; \tau = 1,\dots,M_{u_z} \quad i = 1,\dots,N_n \\
u_\phi^k(x,y,z) &= N_i(y)F^k_{u_\phi\tau}(x,z)q^k_{\phi_{\tau i}} \quad \text{with} \;\; \tau = 1,\dots,M_{u_\phi} \quad i = 1,\dots,N_n
\end{aligned}
\tag{3}
$$

The expansion functions $F^k_{u_x\tau}$, $F^k_{u_y\tau}$, $F^k_{u_z\tau}$, and $F^k_{u_\phi\tau}$ correspond to the generalized displacements $u^k_{x_\tau}$, $u^k_{y_\tau}$, $u^k_{z_\tau}$, and $u^k_{\phi_\tau}$ respectively, providing a basis for approximating these displacement components within the framework. The integers M_{u_x}, M_{u_y}, M_{u_z}, and M_{u_ϕ} denote the number of kinematic expansion terms for each displacement component. In this work, both Taylor and Lagrange expansions are adopted. The shape functions N_i and N_j discretize the solution domain, where N_n indicates the total number of shape functions per element. For comprehensive details on shape function for beams, see [18].
To proceed with the explanation, it is helpful to introduce a compact notation for both the real and virtual systems, as presented below:

$$
u^k_l = N_i F^k_{u_l\tau} q^k_{l_{\tau i}} \quad \text{with} \;\; \tau = 1,\dots,M_{u_l} \;\; \text{and} \;\; i = 1,\dots,N_n \tag{4}
$$

$$
\delta u^k_m = N_j F^k_{u_m s} \delta q^k_{m_{sj}} \quad \text{with} \;\; s = 1,\dots,M_{u_m} \;\; \text{and} \;\; j = 1,\dots,N_n \tag{5}
$$

where l and m can assume the values x, y, z, and ϕ.

3 GOVERNING EQUATIONS AND FINITE ELEMENT MATRICES

The electric field, $\mathbf{E}$, is first expressed as a 3×1 vector quantity:

$$
\mathbf{E}^k = \left\{ \begin{array}{ccc} E^k_x & E^k_y & E^k_z \end{array} \right\}^T = \left\{ \begin{array}{ccc} \partial_x & \partial_y & \partial_z \end{array} \right\}^T \phi^k \tag{6}
$$

The generalized strain vector, $\overline{\boldsymbol{\varepsilon}}$, is expressed in 9×1form as:

$$
\overline{\boldsymbol{\varepsilon}}^k = \left\{ \begin{array}{ccccccccc} \varepsilon^k_{xx} & \varepsilon^k_{yy} & \varepsilon^k_{zz} & \varepsilon^k_{yz} & \varepsilon^k_{xz} & \varepsilon^k_{xy} & E^k_1 & E^k_2 & E^k_3 \end{array} \right\}^T = \overline{\mathbf{D}}\mathbf{u}^k \tag{7}
$$

where $\overline{\mathbf{D}}$ is the matrix of differential operators for small displacements and rotations. For more details, refer to [11, 12]. The coupled electromechanical constitutive relations (stress-charge form) are expressed in matrix notation as:

$$
\begin{aligned}
\boldsymbol{\sigma}^k &= \mathbf{C}^{kE}\boldsymbol{\varepsilon}^k - \mathbf{e}^{kT}\mathbf{E}^k \\
\boldsymbol{D}^k_e &= \mathbf{e}^k\boldsymbol{\varepsilon}^k + \boldsymbol{\chi}^{kS}\mathbf{E}^k
\end{aligned}
\tag{8}
$$

In this formulation, $\boldsymbol{D}^k_e$ indicates the electric displacement vector $\{D^k_x, D^k_y, D^k_z\}^T$, $\boldsymbol{\sigma}^k$ stands for the classical mechanical stress vector, $\mathbf{C}^{kE}$ is the 6×6 matrix for the material coefficients evaluated at a constant electric field, and $\boldsymbol{\varepsilon}^k$ is the strain vector. The 3×3 $\boldsymbol{\chi}^{kS}$ is the dielectric permittivity matrix calculated at constant strain, and the 3×6 $\boldsymbol{e}^k$ is the piezoelectric stiffness coefficient matrix. Their complete expressions can be found in [18, 11, 12]. The generalized 9 $\times$ 1 stress vector can be seen as:

$$\overline{\boldsymbol{\sigma}}^k = \left\{ \begin{array}{ccccccccc} \sigma_{xx}^k & \sigma_{yy}^k & \sigma_{zz}^k & \sigma_{yz}^k & \sigma_{xz}^k & \sigma_{xy}^k & -D_1^k & -D_2^k & -D_3^k \end{array} \right\}^T \tag{9}$$

The constitutive equations is ow rewritten as follows

$$\overline{\boldsymbol{\sigma}}^k = \tilde{\mathbf{H}}^k \overline{\boldsymbol{\varepsilon}}^k \tag{10}$$

where

$$\tilde{\mathbf{H}}^k = \begin{bmatrix} C_{11}^{kE} & C_{12}^{kE} & C_{13}^{kE} & 0 & 0 & C_{16}^{kE} & -e_{11}^k & -e_{21}^k & -e_{31}^k \\ C_{21}^{kE} & C_{22}^{kE} & C_{23}^{kE} & 0 & 0 & C_{26}^{kE} & -e_{12}^k & -e_{22}^k & -e_{32}^k \\ C_{31}^{kE} & C_{32}^{kE} & C_{33}^{kE} & 0 & 0 & C_{36}^{kE} & -e_{13}^k & -e_{23}^k & -e_{33}^k \\ 0 & 0 & 0 & C_{44}^{kE} & C_{45}^{kE} & 0 & -e_{14}^k & -e_{24}^k & -e_{34}^k \\ 0 & 0 & 0 & C_{45}^{kE} & C_{55}^{kE} & 0 & -e_{15}^k & -e_{25}^k & -e_{35}^k \\ C_{61}^{kE} & C_{62}^{kE} & C_{63}^{kE} & 0 & 0 & C_{66}^{kE} & -e_{16}^k & -e_{26}^k & -e_{36}^k \\ e_{11}^k & e_{12}^k & e_{13}^k & e_{14}^k & e_{15}^k & e_{16}^k & \chi_{11}^{kS} & \chi_{12}^{kS} & 0 \\ e_{21}^k & e_{22}^k & e_{23}^k & e_{24}^k & e_{25}^k & e_{26}^k & \chi_{21}^{kS} & \chi_{22}^{kS} & 0 \\ e_{31}^k & e_{32}^k & e_{33}^k & e_{34}^k & e_{35}^k & e_{36}^k & 0 & 0 & \chi_{33}^{kS} \end{bmatrix} \tag{11}$$

Now, it is possible to derive the governing equations from the principle of virtual displacements, which states:

$$\delta L_{int} = \delta L_{ext} \tag{12}$$

For the internal work, δL_{int} is written down as follows:

$$\delta L_{int} = \int_{V^k} \delta \overline{\boldsymbol{\epsilon}}^{kT} \overline{\boldsymbol{\sigma}}^k \mathrm{d}V^k \tag{13}$$

where $\mathrm{d}V^k = \mathrm{d}x^k \mathrm{d}y^k \mathrm{d}z^k$.
Instead, the virtual external work, δL_{ext}, is evaluated as given below:

$$\delta L_{ext} = \int_{V^k} \delta \mathbf{u}^{kT} \mathbf{P}^k \mathrm{d}V^k = \int_{V^k} (\delta u_x^k P_x^k + \delta u_y^k P_y^k + \delta u_z^k P_z^k + \delta u_\phi^k P_\phi^k) \mathrm{d}V^k \tag{14}$$

Through systematic application of the kinematic displacement-strain relations, FE shape function approximations, and the electromechanical constitutive laws, the four coupled governing equations are derived in their final form:

$$\begin{aligned} \delta q_{x_{sj}}^k &: K_{u_x u_x s\tau ji}^k q_{x_{\tau i}}^k + K_{u_x u_y s\tau ji}^k q_{y_{\tau i}}^k + K_{u_x u_z s\tau ji}^k q_{z_{\tau i}}^k + K_{u_x u_\phi s\tau ji}^k q_{\phi_{\tau i}}^k = P_{u_x sj}^k \\ \delta q_{y_{sj}}^k &: K_{u_y u_x s\tau ji}^k q_{x_{\tau i}}^k + K_{u_y u_y s\tau ji}^k q_{y_{\tau i}}^k + K_{u_y u_z s\tau ji}^k q_{z_{\tau i}}^k + K_{u_y u_\phi s\tau ji}^k q_{\phi_{\tau i}}^k = P_{u_y sj}^k \\ \delta q_{z_{sj}} &: K_{u_z u_x s\tau ji}^k q_{x_{\tau i}}^k + K_{u_z u_y s\tau ji}^k q_{y_{\tau i}}^k + K_{u_z u_z s\tau ji}^k q_{z_{\tau i}}^k + K_{u_z u_\phi s\tau ji}^k q_{\phi_{\tau i}}^k = P_{u_x sj}^k \\ \delta q_{\phi_{sj}}^k &: K_{u_\phi u_x s\tau ji}^k q_{x_{\tau i}}^k + K_{u_\phi u_y s\tau ji}^k q_{y_{\tau i}}^k + K_{u_\phi u_z s\tau ji}^k q_{z_{\tau i}}^k + K_{u_\phi u_\phi s\tau ji}^k q_{\phi_{\tau i}}^k = P_{u_\phi sj}^k \end{aligned} \tag{15}$$

This work introduces a novel formulation of the Fundamental Nucleus (FN), where:

- The FNs $K^k_{u_m u_l s\tau ji}$ and $P^k_{u_m sj}$ are single scalar components;
- The theory requires only 16 independent scalar parameters for complete stiffness characterization (and 4 for the load array).

This represents a significant modification compared to traditional CUF implementations [11, 12] that employ 4×4 FN matrix. This contrasts with conventional CUF, which requires all variables to share the same expansion theory, often forcing unnecessary computational. The assembly across all nodes and elements results in the problem:

$$\mathbf{KU} = \mathbf{P} \tag{16}$$

Figure 2 demonstrates the systematic assembly procedure for the global stiffness matrix through

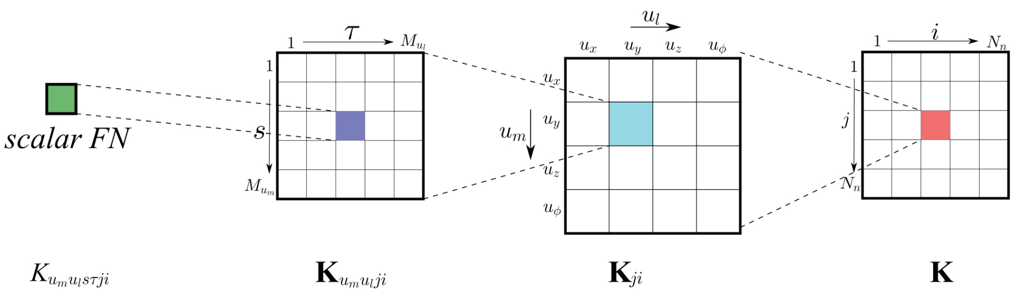

Figure 2: Assembly of the stiffness matrix, starting from the scalar fundamental nuclei.

three expansion stages. The invariant fundamental kernel is first developed through indices s and τ. The resulting submatrix undergoes expansion via displacement component indices u_m and u_l. Final expansion through nodal indices j and i generates the complete structural stiffness matrix.

4 ASSEMBLY

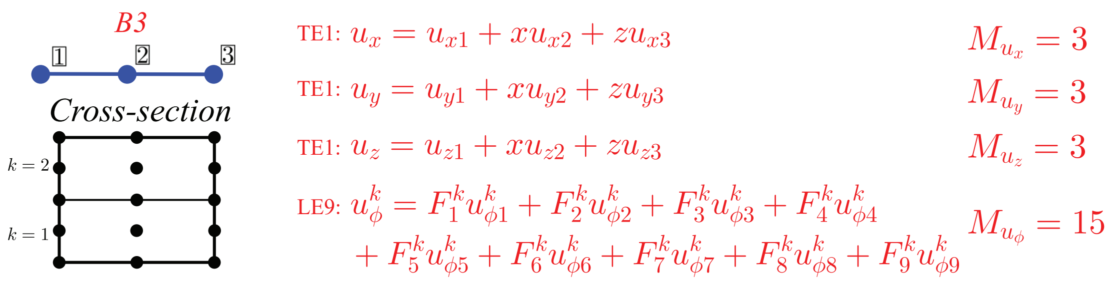

Figure 3: Example of a beam element with a mixed ESL/LW model.

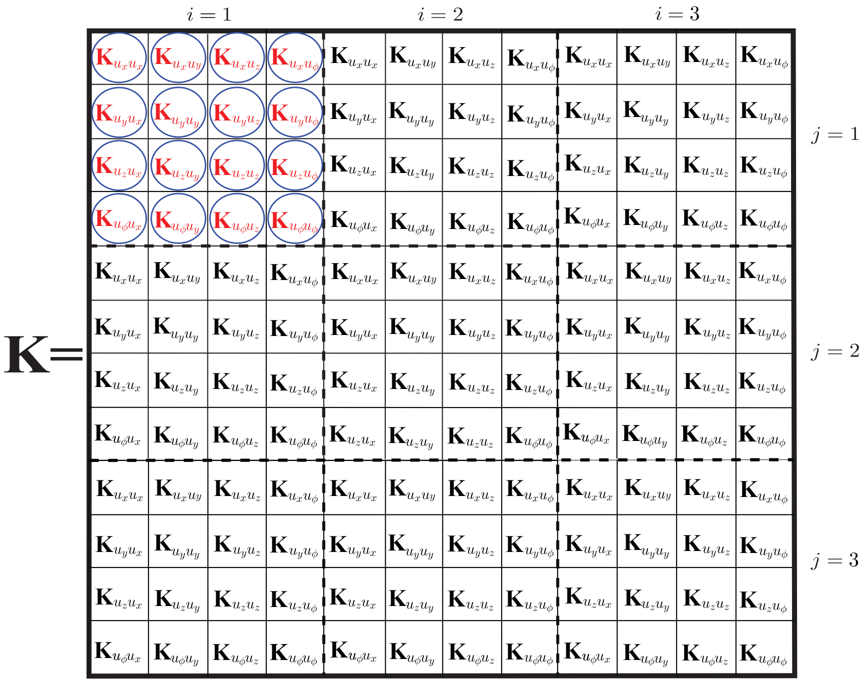

Figure 4: Assembly of the general stiffness matrix with total dimension 72×72.

This section presents the finite element matrix assembly for a multilayered beam element. As a representative example, the three-node element (B3) shown in Fig. 3 is considered, featuring two distinct material layers, a mixed ESL/LW kinematic formulation, and 72 total degrees of freedom. The displacement field employs linear Taylor expansions (TE1) for all components ($M_{u_x} = M_{u_y} = M_{u_z} = 3$), while the electric potential, ϕ, is discretized using two nine-node Lagrange expansions (LE9) with $M_{u_\phi} = 15$.
Figure 4 displays the assembled global stiffness matrix $\mathbf{K}$. While the formulation is presented specifically for the stiffness matrix (for conciseness), the methodology applies equally to the load vector $\mathbf{P}$. This scheme maintains model independence, though the actual matrix dimensions scale with the system's degrees of freedom. The stiffness matrix features a block structure where each sub-matrix $\mathbf{K}_{ji}$ decomposes into sixteen fundamental blocks $\mathbf{K}_{u_m u_l ji}$. For purely mechanical systems, this reduces to nine active sub-matrices, as detailed in Carrera *et al.* [16].

5 RESULTS

This section presents a comprehensive validation study through one canonical benchmarks, evaluating coupled electromechanical bending. The case study investigates a bimorph beam functioning as an actuator.

5.1 Acronym system

In the paper, a coherent acronym system is adopted to identify the structural theories. For instance, in the context of Lagrange-based expansions, the model LE9-LE9-LE9-LE9 indicates that all generalized displacement components are represented using bi-parabolic expansions. The number of Lagrange CUF elements employed for each material layer is explicitly stated. Moreover, mixed ESL/LW theories are utilized, enabling the formulation of refined models such as TE2-TE3-TE2-LE9, where different expansion types and orders are selectively applied to each component.

5.2 Polyvinylidene (PVDF) Bimorph Beam: Actuator Case

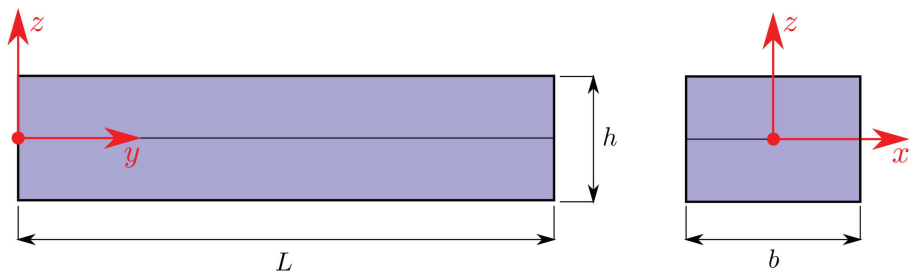

Figure 5: Geometrical properties of the bimorph beam.

A cantilever beam composed of two oppositely polarized Polyvinylidene (PVDF) layers is analyzed. The beam has a total thickness of 1 [mm], a length of 100 [mm], and a width of 5 [mm]. It is fixed on the left end, with an applied electric potential of 1 [V] across its thickness. The material properties are provided in Table 5.2. Note that the bimorph PVDF model excludes the piezoelectric constants e_{33} and e_{15}. The beam geometry is illustrated in Fig. 5. The present results are compared with three literature models. Miglioretti and Carrera [11] employed a uniform CUF-based expansion, while Tzou and Ye [19] used triangular shell elements with mechanical (FOSDT) and electrical degrees of freedom. Additionally, Chee *et al.* [20] implemented Hermitian beam elements with a layer-wise electric potential formulation. The deflection of the cantilever bimorph along its length is illustrated in Fig. 6. The present results demonstrate that it is convenient to use mixed ESL/LW, and they perfectly match the references.

6 CONCLUSIONS

This strategy is particularly effective for complex laminated structures, where different physical fields require varying levels of detail. Numerical analyses confirm the effectiveness of the approach, demonstrating its ability to provide accurate and efficient multi-field simulations. By selecting appropriate kinematic formulations for each field, the proposed method achieves high-fidelity modelling while significantly reducing computational costs. The benchmarks collectively verify the formulation's accuracy across both actuation and sensing configurations.

Table 1: Material properties for bimorph cantilever beam

PVDF		
Elastic modulus	2.00×10^9	Pa
Shear modulus	2.00×10^8	Pa
Mass density	2.00×10^3	Kg m^{-3}
Poisson ratio	0.29	—
e_{31} Piezo	0.046	Cm^{-2}
e_{32} Piezo	0.046	Cm^{-2}
Elec. perm. χ_{11}	1.06×10^{-10}	Fm^{-1}
Elec. perm. χ_{22}	1.06×10^{-10}	Fm^{-1}
Elec. perm. χ_{33}	1.06×10^{-10}	Fm^{-1}

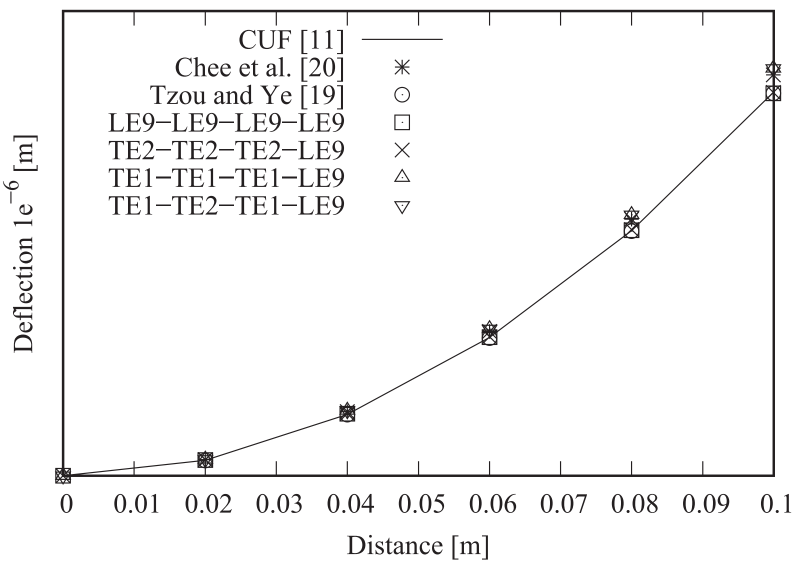

Figure 6: Deflection of the bimorph cantilever along its length.

The proposed method is particularly promising for applications requiring extensive simulations, such as wave propagation studies in health monitoring systems, where computational efficiency is crucial for real-time analysis and large-scale simulations.

REFERENCES

[1] E. F. Crawley and J. de Luis, "Use of piezoelectric actuators as elements of intelligent structures," *AIAA Journal*, vol. 25, no. 10, pp. 1373–1385, 1987. [Online]. Available: https://doi.org/10.2514/3.9792

[2] T. Bailey and J. E. Hubbard, "Distributed piezoelectric-polymer active vibration control of a cantilever beam," *Journal of Guidance, Control, and Dynamics*, vol. 8, no. 5, pp. 605–611, 1985. [Online]. Available: https://doi.org/10.2514/3.20029

[3] D. Robbins and J. Reddy, "Analysis of piezoelectrically actuated beams using a layer-wise displacement theory," *Computers & Structures*, vol. 41, no. 2, pp. 265–279, 1991. [Online]. Available: https://www.sciencedirect.com/science/article/pii/004579499190430T

[4] D. A. Saravanos and P. R. Heyliger, "Mechanics and computational models for laminated piezoelectric beams, plates, and shells," *Applied Mechanics Reviews*, vol. 52, no. 10, pp. 305–320, 10 1999. [Online]. Available: https://doi.org/10.1115/1.3098918

[5] X.-J. Dong, G. Meng, and J.-C. Peng, "Vibration control of piezoelectric smart structures based on system identification technique: Numerical simulation and experimental study," *Journal of Sound and Vibration*, vol. 297, no. 3, pp. 680–693, 2006. [Online]. Available: https://www.sciencedirect.com/science/article/pii/S0022460X06003087

[6] K. Umes and R. Ganguli, "Shape and vibration control of a smart composite plate with matrix cracks," *Smart Materials and Structures*, vol. 18, no. 2, p. 025002, dec 2008. [Online]. Available: https://dx.doi.org/10.1088/0964-1726/18/2/025002

[7] K. Ramesh Kumar and S. Narayanan, "The optimal location of piezoelectric actuators and sensors for vibration control of plates," *Smart Materials and Structures*, vol. 16, no. 6, p. 2680, nov 2007. [Online]. Available: https://dx.doi.org/10.1088/0964-1726/16/6/073

[8] C. Vasques and J. Dias Rodrigues, "Active vibration control of smart piezoelectric beams: Comparison of classical and optimal feedback control strategies," *Computers & Structures*, vol. 84, no. 22, pp. 1402–1414, 2006, composite Adaptive Structures: Modelling and Simulation. [Online]. Available: https://www.sciencedirect.com/science/article/pii/S0045794906000964

[9] J. M. Simões Moita, C. M. Mota Soares, and C. A. Mota Soares, "Active control of forced vibrations in adaptive structures using a higher order model," *Composite Structures*, vol. 71, no. 3, pp. 349–355, 2005, fifth International Conference on Composite Science and Technology. [Online]. Available: https://www.sciencedirect.com/science/article/pii/S0263822305002618

[10] S. Beheshti-Aval, M. Lezgy-Nazargah, P. Vidal, and O. Polit, "A refined sinus finite element model for the analysis of piezoelectric-laminated beams," *Journal of Intelligent Material Systems and Structures*, vol. 22, no. 3, pp. 203–219, 2011. [Online]. Available: https://doi.org/10.1177/1045389X10396955

[11] F. Miglioretti and E. Carrera, "Application of a refined multi-field beam model for the analysis of complex configurations," *Mechanics of Advanced Materials and Structures*, vol. 22, no. 1-2, pp. 52–66, 2015. [Online]. Available: https://doi.org/10.1080/15376494.2014.912365

[12] J. Najd, E. Zappino, E. Carrera, W. Harizi, and Z. Aboura, "A variable kinematic model for the prediction of capacitance variations in embedded PZT sensors," *Journal of Intelligent Material Systems and Structures*, vol. 34, no. 7, pp. 811–824, 2023. [Online]. Available: https://doi.org/10.1177/1045389X221121974

[13] D. Ballhause, M. D'Ottavio, B. Kröplin, and E. Carrera, "A unified formulation to assess multilayered theories for piezoelectric plates," *Computers & Structures*, vol. 83, no. 15, pp. 1217–1235, 2005, modelling of Smart Structures. [Online]. Available: https://www.sciencedirect.com/science/article/pii/S0045794905000271

[14] R. Schardt, "Eine Erweiterung der Technischen Biegetheorie zur Berechnung prismatischer Faltwerke," *Der Stahlbau*, vol. 35, pp. 161–171, 1966.

[15] E. Carrera and D. Scano, "Beam finite element models with node dependent kinematics and arbitrary displacement fields over the cross-section," *Mechanics of Advanced Materials and Structures*, 2025. [Online]. Available: https://doi.org/10.1080/15376494.2024.2434198

[16] E. Carrera, D. Scano, and E. Zappino, "Plate finite elements with arbitrary displacement fields along the thickness," *Finite Elements in Analysis and Design*, vol. 244, p. 104296, 2025. [Online]. Available: https://www.sciencedirect.com/science/article/pii/S0168874X24001902

[17] E. Carrera and D. Scano, "Complete variable kinematics CUF-based multilayered shell elements," in *16th World Congress on Computational Mechanics and 4th Pan American Congress on Computational Mechanics*, July 2024. [Online]. Available: https://www.scipedia.com/public/Carrera_Scano_2024a

[18] K. Bathe, *Finite Element Procedure*. Upper Saddle River, New Jersey, USA: Prentice hall, 1996.

[19] H. S. Tzou and R. Ye, "Analysis of piezoelastic structures with laminated piezoelectric triangle shell elements," *AIAA Journal*, vol. 34, no. 1, pp. 110–115, 1996. [Online]. Available: https://doi.org/10.2514/3.12907

[20] C. Y. K. Chee, L. Tong, and G. P. Steven, "A mixed model for composite beams with piezoelectric actuators and sensors," *Smart Materials and Structures*, vol. 8, no. 3, p. 417, jun 1999. [Online]. Available: https://dx.doi.org/10.1088/0964-1726/8/3/313